J. Fluid Mech. (1995), *vol.* 301, *pp.* 79–107

Parasitic capillary waves: a direct calculation

By MICHAEL S. LONGUET-HIGGINS
Institute for Nonlinear Science, University of California, San Diego, La Jolla, CA 92093-0402, USA

(Received 17 February 1995 and in revised form 22 May 1995)

As in a previous theory (Longuet-Higgins 1963) parasitic capillary waves are considered as a perturbation due to the local action of surface tension forces on an otherwise pure progressive gravity wave. Here the theory is improved by: (i) making use of our more accurate knowledge of the profile of a steep Stokes wave; (ii) taking account of the influence of gravity on the capillary waves themselves, through the effective gravitational acceleration g^* for short waves riding on longer waves.

Nonlinearity in the capillary waves themselves is not included, and certain other approximations are made. Nevertheless, the theory is shown to be in essential agreement with experiments by Cox (1958), Ebuchi, Kawamura & Toba (1987) and Perlin, Lin & Ting (1993).

A principal result is that for gravity waves of a given length $L > 5$ cm there is a critical steepness parameter $(AK)_c$ at which the surface velocity (in a frame of reference moving with the phase-speed) equals the minimum (local) speed of capillary–gravity waves. On *subcritical* gravity waves, with steepness $AK < (AK)_c$, capillary waves may be generated at all points of the wave surface. On supercritical waves, with $AK > (AK)_c$, capillary waves can only be generated in the wave troughs; they are trapped between two caustics near the crests. Generally, the amplitude of the parasitic capillaries is greatest on gravity waves of near critical (but not maximum) steepness.

1. Introduction

There has recently been increased interest in the small-scale structures of wind-waves, partly because of the importance of wavelengths of order 1 cm to the remote-sensing of the sea surface, but more basically because such short waves are believed to affect the large-scale transfers of heat, gases and momentum between the ocean and the atmosphere. Laboratory studies by Jähne & Riemer (1990) have shown that parasitic capillaries generated by short gravity waves, and not directly by the wind, make a significant contribution to the spectrum at these short wavelengths. Since the pioneering experiments of Cox (1958) demonstrating the existence of parasitic capillaries there has been considerable progress in the numerical calculation of the parasitic capillary spectrum, particularly by Watson & McBride (1993). However, the intricacy of their analysis leads one to hope that a simpler and more intuitive approach can be found. The present paper is an attempt to see how far an alternative and more direct treatment (Longuet-Higgins 1963) can be improved so as to yield a physical explanation of the phenomenon.

From the start it is desirable to clarify the nature of the investigation, since some confusion may have been introduced into the subject by a recent paper by Perlin, Lin & Ting (1993). We are not here concerned with the propagation of free, unattenuated ripples over the surface of longer waves, nor with the existence of steady, space periodic

solutions of the inviscid equations of motion such as were found numerically by Schwartz & Vanden-Broeck (1979) and by Chen & Saffman (1979, 1980), and which can be interpreted as short waves propagated on long waves with the same overall phase speed. Neither are we concerned with capillary waves generated at a plunger, or other type of mechanical wavemaker. (For a discussion of the experiments of Perlin *et al.* (1993) see §11 below.) The source of energy for parasitic capillary waves is, by definition, the gravity waves themselves, and not an external source such as the wind or a mechanical wavemaker.

The physical idea underlying the author's (1963) treatment of parasitic capillaries was that on a steep Stokes wave, where the crest is sharper than the trough, the action of surface tension is very uneven, being concentrated mainly near the wave crest. Seen in a reference frame moving with the phase-speed, the Stokes wave appears as a steady (non-uniform) current opposite to the direction of wave propagation. So surface tension should act like a concentrated pressure distribution on the surface of a steady current, producing a train of ripples upstream of the pressure, that is on the forward slope of the Stokes wave. The energy of the ripples was assumed to be subject to viscous decay (Lamb 1932) and to an input of energy by the contraction of the current against the radiation stress. It was shown that the amplitude of the ripples was related to the maximum curvature of the Stokes profile, that is the curvature at the wave crest. The theoretical result was in qualitative agreement with the observations by Cox (1958). However, in deriving the theoretical result use was made of the best theory then available for steep Stokes waves, namely that of Davies (1951). In this theory the curvature at the crest is related ambiguously (and probably incorrectly) to the wave amplitude. Hence one quantitative aspect of the theory was in doubt. Since that time, and especially in the last ten years, greatly improved methods for calculating steep gravity waves have been developed (see §§2 and 3).

Crapper (1970) formulated a somewhat similar theory in which allowance was made for the possible finite steepness of the ripples. He too used Davies' (1951) theory for the underlying Stokes wave. However, he made a highly questionable assumption regarding the energy input to the ripples. Noting that the overall rate of work done by the surface tension T on the fluid equals $T\kappa q_n$ integrated over the surface, where κ is the local curvature and q_n the inward normal velocity, he assumed that all this energy was imparted locally to the ripples. In fact the proportion of energy imparted to the ripples must depend upon the breadth b of the pressure distribution relative to the wavelength (see §4). The breadth is generally greater than the ripple wavelength. For a broad distribution of pressure, the energy imparted to the ripples is relatively small. Thus any quantitative agreement between the predicted and observed ripple amplitudes is surely coincidental (or, as he expressed it, 'the ultimate justification of (27) must therefore depend on experiment').

It is significant that both Longuet-Higgins (1963) and Crapper (1970) ignored the influence of gravity on the short ripples, thereby excluding the possibility of 'blocking' of the short waves at some point near the crest of the gravity wave as described by Phillips (1981) and Shyu & Phillips (1990).

Further experiments designed to test the theory were performed by Chang, Wagner & Yuen (1978). Their conclusion was that the wavelengths of the ripples were fairly well predicted by the theory of Longuet-Higgins (1963), but it was impossible to verify the prediction of their absolute amplitude because of the difficulty of measuring the undisturbed curvature of the wave crest in the presence of short ripples. Ruvinsky & Friedman (1981) pointed out the importance of including gravity as well as capillarity in the dynamics of the ripples, but they ignored the important variations of the effective

gravity g^* along the surface of the gravity wave (see §2). Yermakov, Ruvinsky and Salashin (1988) published experiments correlating the maximum steepness of the ripples with the maximum curvature at the crest of the gravity wave. However, the agreement with theory was not close. Ruvinsky, Feldstein & Freidman (1991) proposed a different numerical method of calculation using a series expansion, and with a new boundary condition, to represent viscous damping of the ripples. A physical interpretation of their analysis has been given by Longuet-Higgins (1992).

In the present paper we aim to extend and improve the analysis in Longuet-Higgins (1963) in the following ways:

(i) By using a modern and accurate method for calculating the profile of steep Stokes waves. This method is described in §§2 and 3. For very steep waves, use is made of the asymptotic theory of the 'almost-highest wave' as developed by Longuet-Higgins & Fox (1977, 1978). In particular this gives a credible theory for the curvature of the profile in the neighbourhood of the crest, and yields conditions for stability.

(ii) By including in the ripple dynamics the effects of particle acceleration in the Stokes waves. This is done by substituting the 'effective gravity' g^* in place of the ordinary gravity g, as in the theory of short gravity waves on longer Stokes waves (Longuet-Higgins 1985*b*, 1987).

This second step makes it possible to calculate the condition for 'blocking' on Stokes waves more accurately (see §6) and to determine, for Stokes waves of a given length L, the critical steepness $(AK)_c$ at which blocking first occurs. Waves for which $AK < (AK)_c$ have no blocking and are called *subcritical*, and those for which $AK > (AK)_c$ and blocking occurs are called *supercritical*. The generation of parasitic capillaries on a subcritical wave is calculated in §7, on a supercritical wave in §8. In the latter case it appears there may be trapping of short-wave energy between two blocking points, or caustics, in the same wave trough. In either case it is found that the ripple amplitude tends to increase as the critical wave steepness is approached, either from above or below; apparently the ripples are highly sensitive to the steepness of the gravity wave in this neighbourhood. The implications of this phenomenon for the damping of gravity waves and for theories of wave generation by wind are discussed in §13.

In §§10–12 we compare the present theory with the laboratory experiments by Cox (1958), Ebuchi *et al.* (1987) and Perlin *et al.* (1993) and show that they are in essential agreement.

2. Stokes waves of finite amplitude

We begin with the improved calculation of pure gravity waves on deep water. A quick and accurate technique was developed by Longuet-Higgins (1985*a*). The wavelength being taken as 2π, the free surface is expressed parametrically by

$$\left.\begin{aligned} y &= \tfrac{1}{2}A_0 + \sum_{n=1}^{\infty} A_n \cos n\theta, \\ x &= \theta + \sum_{n=1}^{\infty} A_n \sin n\theta. \end{aligned}\right\} \tag{2.1}$$

The coefficients A_n are known to satisfy a certain set of quadratic relations. These may be solved numerically for a given value of the wave steepness AK where K is the wavenumber (here $K = 1$) and A is the wave amplitude:

$$A = A_1 + A_3 + A_5 + \ldots. \tag{2.2}$$

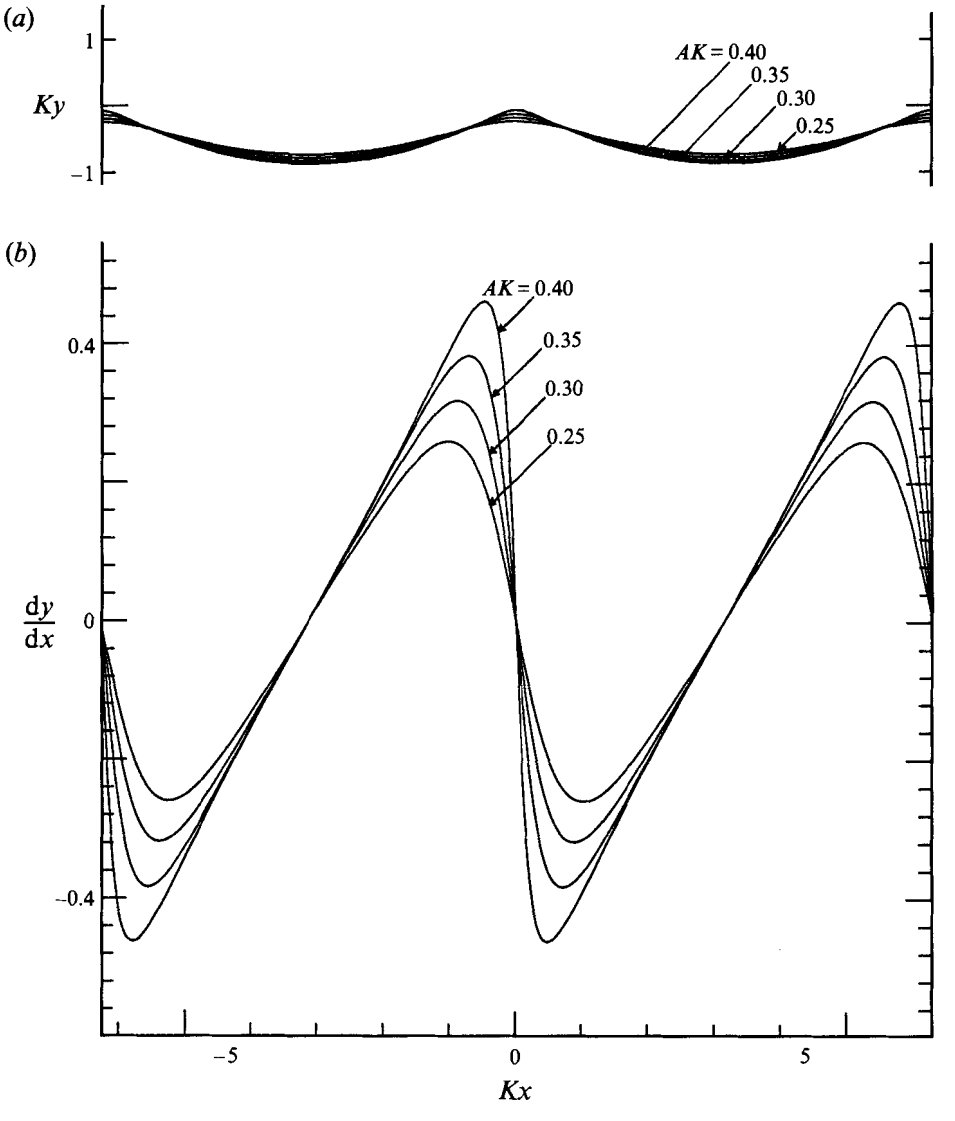

FIGURE 1. Stokes waves on deep water. Wavelength = 2π. Steepness $AK = 0.25$, 0.30, 0.35 and 0.40. (*a*) Surface profiles and (*b*) surface gradient.

Examples of profiles calculated in this way for $AK = 0.25$, 0.30, 0.35 and 0.40 are shown in figure 1 (*a*), and in figure 1 (*b*) we show the corresponding surface slopes. We see that the pattern of slopes tends to become 'saw-toothed' as the steepness AK increases.

For calculating the parasitic capillaries we shall need

(i) the particle velocity U at the free surface in a frame of reference moving with the phase-speed c;

(ii) the curvature κ of the free surface which determines the additional stress $T\kappa$ due to surface tension;

(iii) the effective value g^* of gravity felt by the short waves, that is to say

$$g^* = g\cos\alpha - \kappa U^2, \tag{2.3}$$

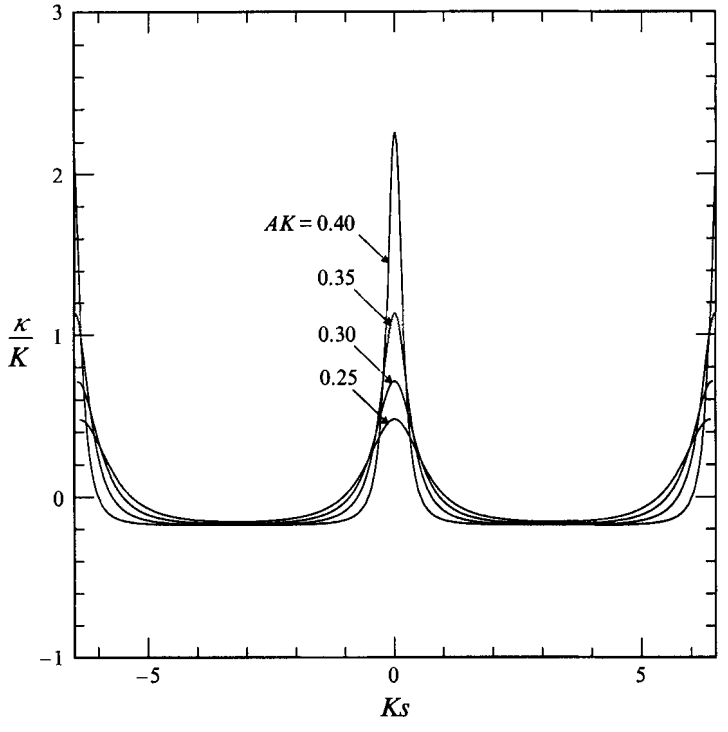

FIGURE 2. Curvature κ of the wave profiles in figure 1, as a function of the arclength s.

where α is the angle of tilt of the surface. The term κU^2 represents the acceleration of a fluid particle normal to the surface.

To find (i) we may simply use Bernoulli's equation

$$U^2 = -2gy, \tag{2.4}$$

since in the representation (2.1) the origin is chosen so that the arbitrary constant vanishes. To find κ we may use

$$\kappa = (x_{\theta\theta} y_\theta - y_{\theta\theta} x_\theta)/(x_\theta^2 + y_\theta^2)^{3/2}, \tag{2.5}$$

where a suffix denotes differentiation; κ is taken as positive when the surface curves downwards. Thirdly, we have

$$\cos\alpha = x_\theta/(x_\theta^2 + y_\theta^2)^{1/2}. \tag{2.6}$$

In figures 2 and 3, κ and g^* are plotted against the arclength s measured along the surface from the crest ($s = 0$). It will be seen how in the steeper waves the curvature becomes concentrated in a very narrow region round the crest, whereas in the wave trough the curvature is almost constant (and negative). The total area under each curve vanishes since

$$\int \kappa \, ds = \int \frac{d\alpha}{ds} ds = [\alpha] = 0, \tag{2.7}$$

when the integral is taken over one wavelength.

The values of κ and g^* at the wave crest are given in table 1 for selected values of AK. The maximum surface gradient is also given.

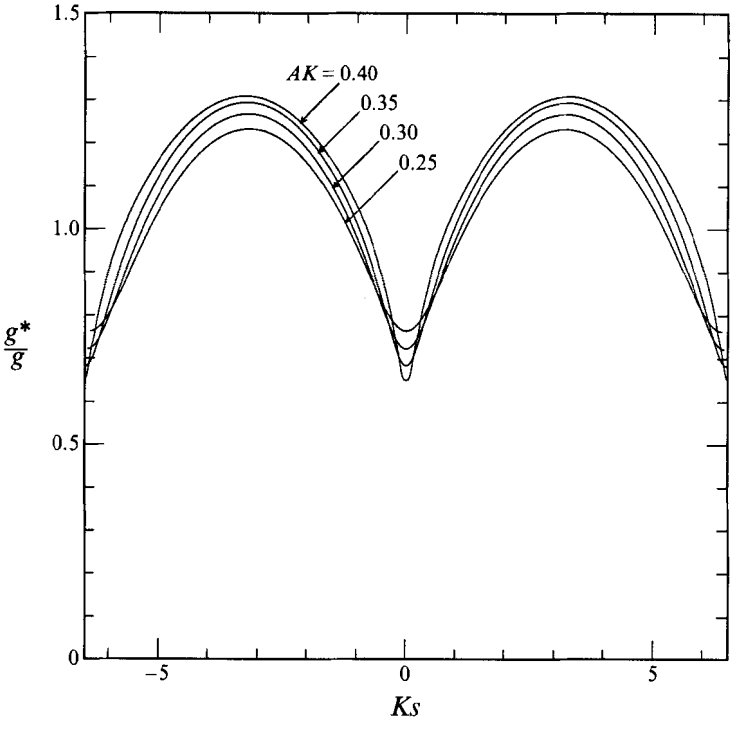

FIGURE 3. The effective gravity g^* for particles at the surface of Stokes waves, as a function of the arclength s.

AK	$(\mathrm{d}y/\mathrm{d}x)_{max}$	α_{max}(deg.)	$(K/g)U_0$	ϵ	κ_0/K	g_0'/g
0.0000	0.0000	0.00	1.0000	0.7071	0.0000	1.0000
0.0500	0.0501	2.87	0.9487	0.6708	0.0554	0.9501
0.1000	0.1005	5.74	0.8944	0.6324	0.1238	0.9009
0.1500	0.1518	8.63	0.8364	0.5914	0.2101	0.8530
0.2000	0.2044	11.55	0.7736	0.5470	0.3226	0.8070
0.2500	0.2593	14.54	0.7043	0.4980	0.4777	0.7630
0.3000	0.3177	17.63	0.6251	0.4420	0.7124	0.7216
0.3500	0.3825	20.93	0.5291	0.3742	1.1339	0.6825
0.4000	0.4622	24.81	0.3942	0.2782	2.2554	0.6496
0.4432	0.5860	30.37	0.0000	0.0000	∞	0.612

TABLE 1. Parameters of Stokes waves, at different values of the wave steepness AK

3. Asymptotic theory for steep waves

When the wave steepness AK approaches its limiting value

$$(AK)_{max} = 0.4432, \tag{3.1}$$

the method of calculation described in §2 loses accuracy, but may be supplemented by an asymptotic method due to Longuet-Higgins & Fox (1977, 1978). This becomes applicable when

$$\epsilon^2 = \frac{U_0^2 K}{2g} \ll 1, \tag{3.2}$$

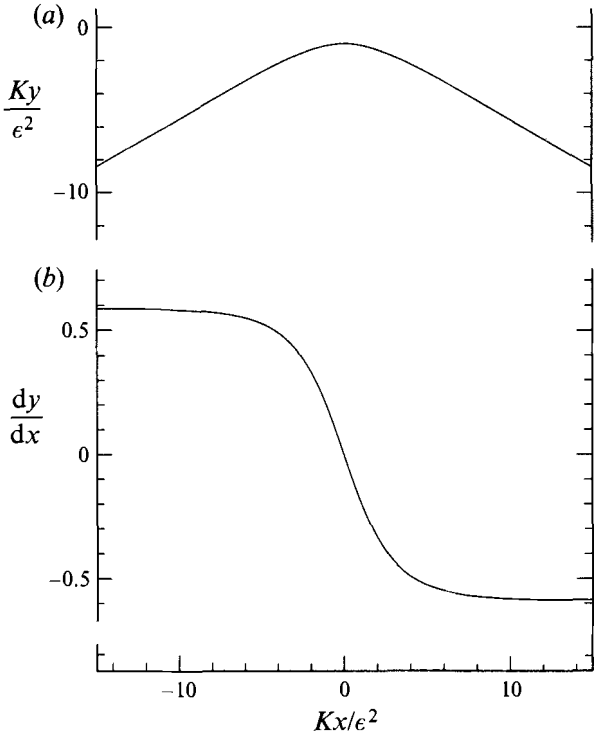

FIGURE 4. Limiting form of a wave crest, from Longuet-Higgins & Fox (1977): (*a*) surface elevation and (*b*) surface slope.

U_0 being the particle speed at the crest in the moving frame of reference. It can be shown that ϵ is related to the wave steepness AK by

$$(AK)_{max} - AK = 0.5\epsilon^2 + O(\epsilon^3), \tag{3.3}$$

(see Longuet-Higgins & Fox 1978, §5).

It is shown by Longuet-Higgins & Fox (1977) that as $\epsilon \to 0$ and $AK \to (AK)_{max}$ the profile of the wave crest approaches a certain limiting form – the 'almost-highest' wave (see figure 4). The limiting form is valid within a distance of order ϵ^2 from the rest. The particle velocity at the crest itself is found from (3.2) to be

$$U_0 = \epsilon(2g/K)^{1/2}. \tag{3.4}$$

In figure 5 we show the surface curvature κ as a function of the arclength s. The radius of curvature at the crest is $5.155\epsilon^2/K$. This leads to a value of the effective gravity g^* given by

$$g^* = 0.612g \tag{3.5}$$

at the crest, independently of ϵ. It has been shown by Longuet-Higgins, Cleaver & Fox (1994) that the crest of a steady gravity wave becomes unstable when ϵ is less than a certain value (see their figure 5) and that this probably corresponds to the lowest superharmonic instability of a Stokes wave at $AK = 0.4292$ (the lowest energy maximum), that is when $\epsilon^2 = 0.028$ ($\epsilon = 0.167$). Hence the theory is not valid beyond this point. In practice, it is likely that a gravity wave crest is unstable to finite-amplitude perturbations at a steepness somewhat below $AK = 0.4292$.

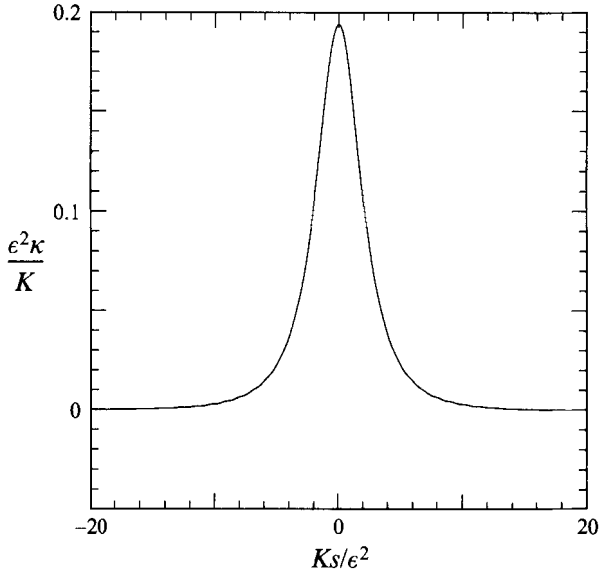

FIGURE 5. Surface curvature κ for the almost-highest wave, as a function of the arclength s.

4. Capillary–gravity waves due to pressure on a uniform stream

It will be helpful to consider first the surface displacement due to a continuous distribution of pressure acting on the surface of a uniform stream which moves to the right with speed U, as in figure 6. Relative to the stream, any steady waves of small slope must have a wavenumber k related to U by the linear dispersion relation

$$Tk^2 - U^2k + g = 0. \tag{4.1}$$

There are two distinct regimes, according to whether

$$\Delta = U^4 - 4gT \tag{4.2}$$

is positive or negative. If $\Delta > 0$, equation (4.1) shows there are two real wavenumbers

$$k_1, k_2 = \frac{1}{2T}(U^2 \pm (U^4 - 4gT)^{1/2}). \tag{4.3}$$

We call k_1 and k_2 the capillary (or capillary–gravity) and the gravity (or gravity–capillary) wavenumbers respectively.

As shown by Lamb (1932, §271) a pressure distribution $P\delta(x)$ concentrated at $x = 0$ gives rise to a surface displacement

$$\zeta(x) = \frac{-2P}{T(k_1 - k_2)} \times \begin{Bmatrix} \sin k_1 x, & x < 0 \\ \sin k_2 x, & x > 0 \end{Bmatrix} + \frac{2P}{T(k_1 - k_2)} F(x) \tag{4.4}$$

where

$$F(x) = \int_0^\infty \left(\frac{\cos kx}{k + k_1} - \frac{\cos kx}{k + k_2} \right) \mathrm{d}k, \quad x > 0 \tag{4.5}$$

with a similar expression for $F(x)$ when $x < 0$. Numerical calculation (see Lamb 1932, §271) shows that $F(x)$ is small except possibly close to the origin (see figure 6).

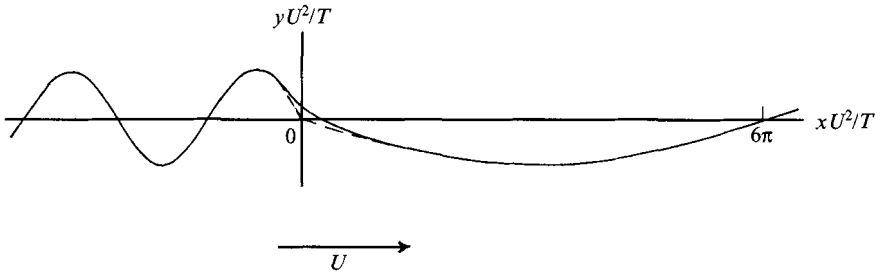

FIGURE 6. Surface disturbance due to a line-pressure acting at $x = 0$ on a uniform stream, when $k_1/k_2 = 5$. The broken line represents the sine-wave part of (4.4). [After Lamb 1932.]

Thus we see the disturbance consists essentially of two systems of waves of equal amplitude

$$a = \frac{2P}{T(k_1 - k_2)} = \frac{2P}{(U^4 - gT)^{1/2}} = \frac{2P}{\Delta^{1/2}}, \tag{4.6}$$

with the capillary waves upstream and the gravity waves downstream of the origin.

Now consider the disturbance due to a distributed pressure $p_s(x)$ acting on the free surface. In general we can consider $p_s(x)$ as the sum of a distribution of point-pressures, so that by (4.4) the capillary-wave part of the solution can be expressed as

$$\zeta(x) = \int_x^\infty \frac{2p_s(x')}{\Delta^{1/2}} \sin k_1(x' - x)\, \mathrm{d}x'. \tag{4.7}$$

Suppose for example that the pressure distribution $p_s(x)$ is given by

$$p_s(x) = \frac{P}{\pi} \frac{b}{b^2 + x^2}. \tag{4.8}$$

When the breadth b of this distribution is small, $p_s(x)$ becomes $P\delta(x)$ as before. Then we shall have

$$\zeta(x) = \frac{2Pb}{\pi\Delta^{1/2}} \int_x^\infty \frac{\sin k_1(x' - x)}{b^2 + x'^2} \mathrm{d}x'. \tag{4.9}$$

At upstream distances x large compared to the breadth b of the pressure pattern, the lower limit of integration in (4.9) can be replaced by $-\infty$ so that

$$\zeta(-\infty) = \frac{2Pb}{\pi\Delta^{1/2}} \int_{-\infty}^\infty \frac{\sin k_1(x' - x)}{x'^2 + b^2} \mathrm{d}x' \tag{4.10}$$

$$= \frac{-2\mathrm{P}}{\Delta^{1/2}} \exp(-bk_1) \sin k_1 x. \tag{4.11}$$

Lamb (1932, §271) derives the same result in a different way. One consequence of (4.11) is that the energy imparted to the capillary wavetrain is proportional to $\exp(-2bk_1)$ and depends strongly on the ratio of the breadth of the pressure distribution to the wavelength of the capillary waves. When $bk_1 > 2$, say, the proportion of energy is very small. This is contrary to the assumption made by Crapper (1970) that all the available energy from surface tension goes into capillary waves. We may say that the smoothness of the pressure distribution will tend to iron out the capillary waves so that only a small proportion of the available energy goes into them.

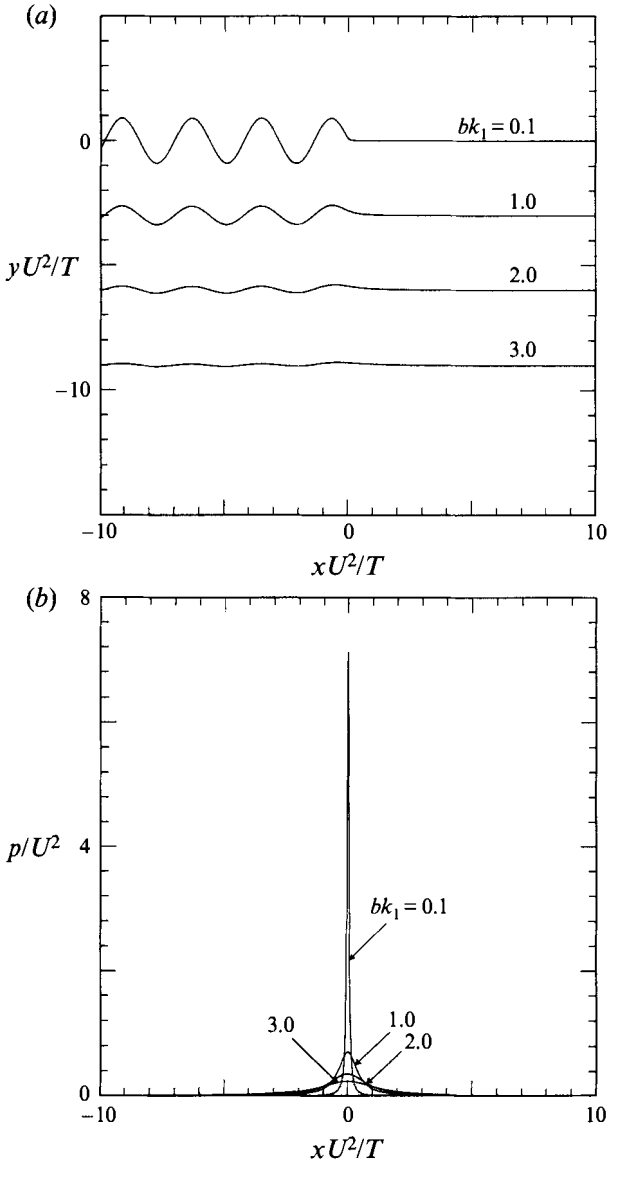

FIGURE 7. Capillary waves due to a pressure distribution $p_s = \pi^{-1}Tb/(b^2+x^2)$ acting on a uniform stream of speed U, when $4gT/U^2 = \frac{5}{9}$ and when $bk_1 = 0.1$, 1.0, 2.0 and 3.0. (*a*) Surface displacement, (*b*) pressure distribution.

Some examples of the surface elevation $\zeta(x)$ as given by (4.9) are shown in figure 7, in the typical case $k_1 = 5k_2$, that is $4gT/U^4 = \frac{5}{9}$, and when $bk_1 = 0.1$, 1, 2 and 3, respectively. The strong dependence of the amplitude on bk_1 is evident.

There will of course be an expression similar to (4.9) for the gravity waves generated by $p_s(x)$, but this is ignored for two reasons:

(i) The wavelength of the gravity waves is generally much greater than that of the corresponding capillary waves. Indeed when we come to consider wave generation by pressures near the crest of Stokes waves (see §6) the corresponding gravity waves are comparable in length to the original Stokes wave and they cannot be considered any

more as short waves propagated over long waves. Though there will undoubtedly be some effect on the Stokes wave, such as a slight change in phase-speed and the generation of some forced higher harmonics, these must be obtained by a different method.

(ii) In many observations the quantity measured is the surface slope rather than the vertical displacement of the free surface. Because of their short wavelength the capillary waves make a relatively larger contribution to the surface slope.

When on the other hand $\Delta < 0$, (4.2) has no real roots, and the displacement ζ tends to zero rapidly with increasing $|x|$.

5. Capillary–gravity waves from a point-source on a non-uniform stream

We shall now consider the generation of capillary–gravity waves by a distribution of pressure acting on a non-uniform current $U(x)$, neglecting at first any deviation of the undisturbed surface from the plane $y = 0$. It is assumed that the current varies sufficiently gradually with x that locally the waves appear as on a uniform stream. A necessary condition is that

$$\frac{\partial U}{\partial x} \ll kU, \tag{5.1}$$

where k is the local wavenumber. In this section it is also assumed that $U^4 > 4gT$ everywhere.

Under this assumption, the value of k for capillary–gravity waves will be given by (4.3), with $k = k_1$. It is convenient to define the local phase θ of the wave by $k = \mathrm{d}\theta/\mathrm{d}x$, hence

$$\theta = \int k \,\mathrm{d}x = \int \frac{k}{U} \mathrm{d}\phi, \tag{5.2}$$

where ϕ is the velocity potential in the undisturbed flow. The surface displacement due to a point-pressure $P\delta(x-x')$ applied at the point $x' > x$ will be given locally by

$$\zeta(x) = a' \sin(\theta' - \theta) \quad (\theta' > \theta), \tag{5.3}$$

where

$$a' = \frac{2P}{(U'^4 - 4gT)^{1/2}}, \quad U' = U(x'), \tag{5.4}$$

as in §4. To find the amplitude at points x not close to x' we may use the principle of action conservation as follows.

The wave amplitude a is related to the energy density E by

$$a^2 = \frac{2E}{g + Tk^2}. \tag{5.5}$$

The wave action density A is defined by

$$A = E/\sigma, \tag{5.6}$$

where σ is the radian frequency, given by $\sigma^2 = gk + Tk^3$. Also, since the waves are steady in a frame moving with speed U, $\sigma/k = U$. So from (5.5) and (5.6)

$$a^2 = \frac{2E}{\sigma^2/k} = \frac{2E}{\sigma U} = \frac{2A}{U}. \tag{5.7}$$

Now if viscous dissipation is taken into account the differential equation for A takes the form

$$\frac{\partial}{\partial x}[A(U-c_g)]+4\nu k^2 A = 0, \tag{5.8}$$

where c_g is the group-velocity and ν the kinematic viscosity (see Shyu & Phillips 1990). By convention we take c_g to be positive, so that $c_g > U$. To solve (5.8) write

$$B = A(c_g-U), \tag{5.9}$$

so that (5.8) becomes

$$\frac{\partial B}{\partial x} = \frac{4\nu k^2}{(c_g-U)}B, \tag{5.10}$$

hence

$$B = B'\exp\left(\int \frac{4\nu k^2}{c_g-U}\mathrm{d}x\right), \tag{5.11}$$

where B' is a constant. Altogether then

$$a^2 = \frac{2B'}{U(c_g-U)}\exp\left(\int \frac{4\nu k^2}{U(c_g-U)}\mathrm{d}\phi\right), \tag{5.12}$$

since $\mathrm{d}x = \mathrm{d}\phi/U$ where ϕ is the velocity potential. However, from the relation

$$\sigma - kU = 0, \tag{5.13}$$

we have, on differentiation,

$$\left(\frac{\mathrm{d}\sigma}{\mathrm{d}k}-U\right)-k\frac{\mathrm{d}U}{\mathrm{d}k} = 0. \tag{5.14}$$

Since $\mathrm{d}\sigma/\mathrm{d}k = c_g$ it follows that

$$U(c_g-U) = Uk\,\mathrm{d}U/\mathrm{d}k, \tag{5.15}$$

but from (4.3) we can easily find

$$Uk\,\mathrm{d}U/\mathrm{d}k = \tfrac{1}{2}(U^4-4gT)^{1/2}. \tag{5.16}$$

On substituting in (5.12) we have

$$a^2 = \frac{4B'}{(U^4-4gT)^{1/2}}\exp\left(\int^{\phi}\frac{8\nu k^2}{(U^4-4gT)^{1/2}}\mathrm{d}\phi\right). \tag{5.17}$$

Now dividing by the value of a^2 at $\phi = \phi'$ and taking the square root we obtain

$$\frac{a}{a'} = \frac{D'}{D}\exp\left(\int_{\phi'}^{\phi}\frac{4\nu k^2}{D^2}\mathrm{d}\phi\right), \tag{5.18}$$

where for brevity we have written

$$D(\phi) = (U^4-4gT)^{1/4}, \quad D' = D(\phi'). \tag{5.19}$$

Altogether from (5.3), (5.4) and (5.18) we find for the displacement ζ due to a point-pressure $P\delta(x-x')$ at $x' > x$:

$$\zeta(\phi) = \frac{2P}{D(\phi)\,D(\phi')}\frac{F(\phi)}{F(\phi')}\sin(\theta'-\theta), \tag{5.20}$$

where
$$F(\phi) = \exp\left(\int_0^\phi \frac{4\nu k^2}{D^2}\,\mathrm{d}\phi\right). \tag{5.21}$$

It is simple to generalize this result to a continuous distribution of pressure $p_s(x)$ acting on the surface of the stream. We simply add the contributions for each point x' downstream of the point x to give

$$\zeta(x) = \int_x^\infty \frac{2p_s(x')}{D(\phi)\,D(\phi')}\frac{F(\phi)}{F(\phi')}\sin(\theta'-\theta)\,\mathrm{d}x'. \tag{5.22}$$

6. The critical wave steepness

We propose now to calculate the capillary–gravity waves generated by the surface-tension pressure $T\kappa$ acting on the surface of free Stokes waves. (The curvature κ has already been found in §§2 and 3.) We suppose the waves travel to the left (x decreasing). By taking a frame of reference moving with the phase speed, the wave is reduced to a steady flow to the right. The speed of the current at the surface (and tangential to it) will be denoted by $U(s)$ where s is the arclength measured from a wave crest. The effect of the surface curvature κ on the propagation of the short waves will be ignored, except that the gravitational acceleration g is replaced everywhere by $g^*(s)$, see equation (2.3). Clearly there are two situations, corresponding to

$$\Delta^* = U^4 - 4g^*T \gtrless 0. \tag{6.1}$$

These we shall call 'resonant' and 'non-resonant', respectively. In the resonant case, k_1 is real, so propagating capillary waves can exist. In the non-resonant case they cannot. For Stokes waves of low amplitude every part of the surface is resonant, but for every Stokes wave of given length, as the steepness AK is increased a part of the surface near the crest becomes non-resonant. At the point where $\Delta^* = 0$ we may say the short capillary–gravity waves are 'blocked' (see Phillips 1981; Shyu & Phillips 1990).

To illustrate the behaviour of the wavenumber k_1 and k_2 in the two cases we show in figure 8 two examples of the local wavenumber k_1 plotted against the arclength s. In both cases the wavelength L equals 8.0 cm. In figure 8(a) the wave is completely resonant; short waves may exist at all points of the surface, and energy may be received at any point from any other point.

In figure 8(b) waves are excluded from the wave crest, and may exist only in a certain range AB centred on the wave trough. The points A and B are wave caustics, or blocking points, and the capillary–gravity waves are trapped between A and B.

The critical steepness $(AK)_c$ of Stokes waves is the value of AK for which steady capillary–gravity waves become blocked. For a given wavelength L of the Stokes waves it is easy to find $(AK)_c$ by the method of §4. Some points calculated in this way are shown by the full line in figure 9.

It will be seen that $(AK)_c$ increases monotonically with L. For large values of L we may derive an asymptote from the analytic expressions given in §3. Thus, since

$$U_0^4 = 4\epsilon^4(g/K)^2, \quad g_0^*/g = 0.612, \tag{6.2}$$

(where a suffix 0 denotes the value at the crest $\phi = 0$) we see from (6.1) that Δ_0^* vanishes when

$$\epsilon^4 = 0.612\left(\frac{TK^2}{g}\right), \tag{6.3}$$

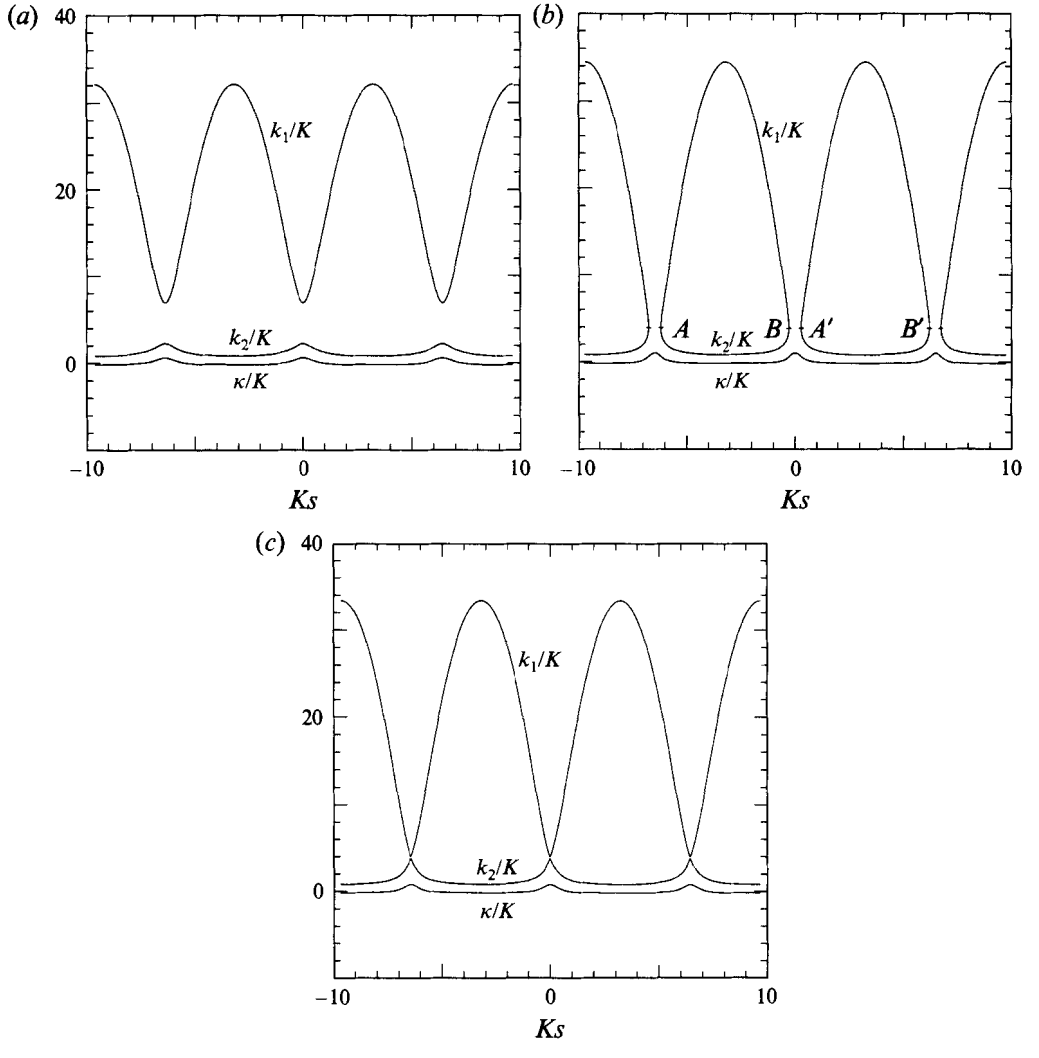

FIGURE 8. Graphs of the wavenumbers k_1 and k_2 when $L = 8.0$ cm. The surface curvature κ is shown on the same scale. (*a*) $AK = 0.28$ (subcritical), (*b*) $AK = 0.34$ (supercritical), (*c*) $AK = 0.311$ (critical).

or by (3.3) when

$$(AK)_{max} - AK \sim 0.391\left(\frac{TK^2}{g}\right)^{1/2}. \tag{6.4}$$

Hence, if T, g and $L = 2\pi/K$ are given in c.g.s. units, we have

$$(AK)_c = 0.4432 - 0.679L^{-1}. \tag{6.5}$$

This asymptote is represented by the upper broken curve in figure 9.

Less rigorously, we may find a rough approximation for lower values of L. For, from the linearized theory of waves of small steepness we have

$$U_0 = C - A\Sigma = C(1 - AK), \tag{6.6}$$

$$g_0^* = g - A\Sigma^2 = g(1 - AK), \tag{6.7}$$

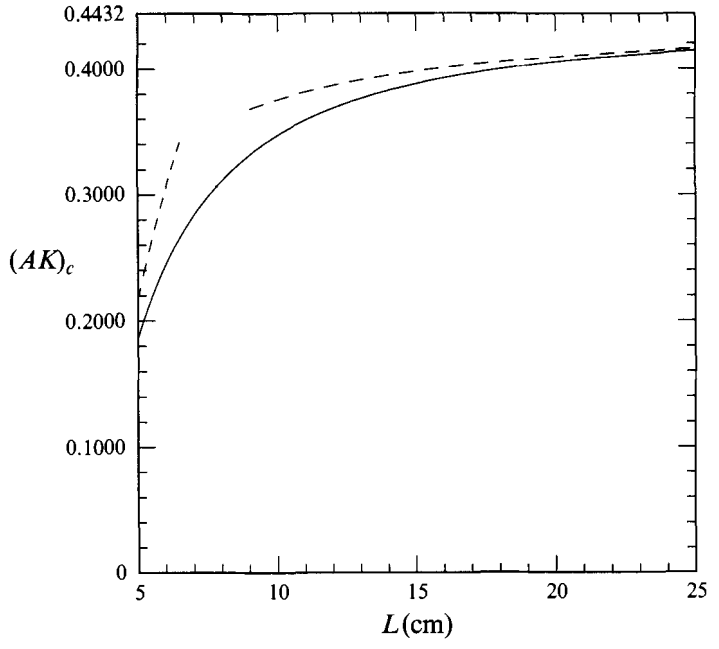

FIGURE 9. Graph of the critical wave steepness $(AK)_c$ for blocking of capillary–gravity waves, as a function of the wavelength L of the Stokes waves. Broken lines represent the two asymptotes (6.5) and (6.9).

where C and Σ denote the speed and the radian frequency of the basic wave. Substitution in the condition $\Delta^* = 0$ gives

$$(1-AK)^3 = \frac{4TK^2}{g}. \tag{6.8}$$

Hence, for the critical steepness we have

$$(AK)_c = 1-\left(\frac{4TK^2}{g}\right)^{1/3} = 1-2.29L^{-2/3}, \tag{6.9}$$

L being in cm. This second approximation is shown by the lower dashed curve in figure 9.

It will be convenient to say that Stokes waves whose steepness is less than $(AK)_c$ are 'subcritical', while those with steepness greater than $(AK)_c$ are 'supercritical'.

7. Generation of capillary–gravity waves on a Stokes wave: subcritical case

In the next two sections we shall calculate the generation of parasitic capillary waves by the local action of the surface tension force $T\kappa$ on a Stokes wave.

We suppose that the capillary–gravity waves are sufficiently short that they are propagated on the Stokes wave as on a gradually-varying non-uniform stream. The analysis of §5 will then apply, except that the horizontal coordinate x must be replaced by the distance s measured along the free surface, and g must be replaced by the effective gravity g^*. At each point s the surface tension exerts a pressure $p_s = T\kappa(s)$. Hence, as in §4, we may write down the normal displacement ζ due to the pressure

applied at all points s' downstream of an arbitrary fixed point s. If the surface is resonant at all points on the wave, this gives, as in (5.22),

$$\zeta(s) = \int_s^\infty \frac{2T\kappa(s')}{D(\phi)\,D(\phi')}\frac{F(\phi)}{F(\phi')}\sin(\theta'-\theta)\,\mathrm{d}s', \tag{7.1}$$

where

$$\left.\begin{aligned} D(\phi) &= (U^4-4g^*T)^{1/4}, \\ F(\phi) &= \exp\left(4\nu\int_0^\phi k^2/D^2\,\mathrm{d}\phi\right), \\ \theta(\phi) &= \int_0^\phi k/U\,\mathrm{d}\phi. \end{aligned}\right\} \tag{7.2}$$

and $k = (U^2+D^2)/2T$. For computation it is convenient to separate the integral into two parts by expanding the term $\sin(\theta'-\theta)$ and replacing $\mathrm{d}s'$ by $\mathrm{d}\phi'/U(\phi')$. Thus

$$\zeta(s) = 2T\frac{F(\phi)}{D(\phi)}[H(\phi)\cos\theta - G(\phi)\sin\theta], \tag{7.3}$$

where

$$\left.\begin{aligned} G(\phi) &= \int_\phi^\infty \frac{\kappa(\phi')}{D(\phi')\,F(\phi')\,U(\phi')}\cos\theta'\,\mathrm{d}\phi', \\ H(\phi) &= \int_\phi^\infty \frac{\kappa(\phi')}{D(\phi')\,F(\phi')\,U(\phi')}\sin\theta'\,\mathrm{d}\phi', \end{aligned}\right\} \tag{7.4}$$

Note that the function $F(\phi)$ of (7.2) need only be computed once, and may then be used both inside and outside the integrals (7.4).

The nature of the solution is best seen by imagining the water surface to be straightened out into a plane. The curvature $\kappa(s)$ then vanishes, but we may apply a surface pressure over some localized region, say near $s = 0$ (corresponding to a wave crest). For example, take p_s to be given by (4.8) with $P = T$. This is the pressure that would be exerted by a surface curvature

$$\kappa(s) = \frac{1}{\pi}\frac{b}{b^2+s^2}, \tag{7.5}$$

with total change of surface slope

$$\Delta\alpha = \int_{-\infty}^\infty \kappa(s)\,\mathrm{d}s = 1\,\mathrm{rad}. \tag{7.6}$$

Figure 10(a) shows the surface displacement $\zeta(x)$ given by (7.3) in the typical case $L = 6.82$ cm, $AK = 0.217$ and $Kb = 0.1$ (the width b is about $\frac{1}{60}$th of the wavelength (L). The capillary–gravity wave train is mainly upstream of the origin, but the wavelength $2\pi/k$ is greatest near the wave crests. The amplitude decays with distance upstream on the whole, but with a tendency to be greatest at the wave crests, as a result of the radiation stress. The energy from the wave crest at $s = 0$ spills over onto the rear and forward slope of the next crest upstream ($Ks = -2\pi$). The nearest crest downstream ($Ks = 2\pi$) contributes very little.

Figure 10(b) shows a similar picture when the pressure distribution is broadened to $Kb = 1.0$, on the same scale. The peak ripple amplitude is reduced by a factor of more than 10. Moreover, the ripple amplitude generally is reduced relative to the first peak.

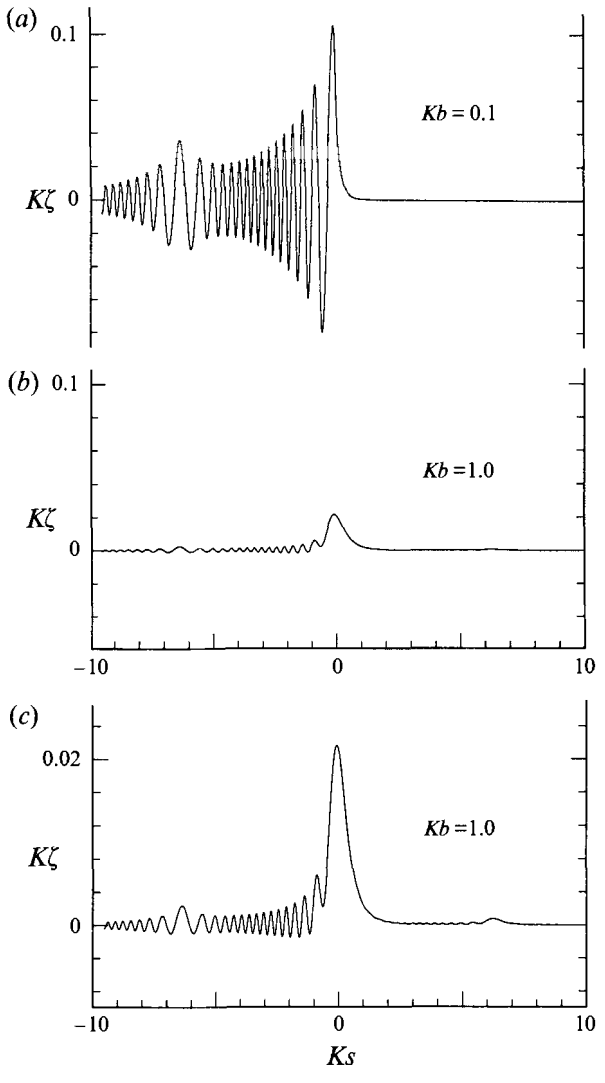

FIGURE 10. Surface displacement $\zeta(s)$ induced by the localized pressure distribution (7.5) on a wave surface which has been straightened out, but with k and g^* appropriate for a Stokes wave having $L = 6.82$ cm, $AK = 0.217$. (*a*) $Kb = 0.1$; (*b*) $Kb = 1.0$; (*c*) as in (*b*) but vertical scale enlarged.

A vertical enlargement (figure 10*c*) shows that there is now a slight contribution from the downstream 'crest' at $Ks = 2\pi$; the pressure $p_s(s)$ extends out to this distance.

Returning now to the curved surface of a Stokes wave, we show in figure 11(*a*) the normal displacement $\zeta(s)$ in the case corresponding to figure 8(*a*) where $L = 8.0$ cm. Integration has been started from a point (∞) two wavelengths to the right. There is some slight overlap between the contributions from adjacent waves, but after one wave the curve settles down to a steady state. Evidently the ripples are most marked on the forward face of the wave. Figure 11(*b*) shows the profile of the perturbed Stokes wave.

Since many optical techniques are designed to measure the surface slope rather than the elevation directly, we show in figure 11(*c*) the corresponding slope $\mathrm{d}y/\mathrm{d}x$ as a function of x. The contribution of the short ripples is now magnified relative to that of the underlying gravity wave.

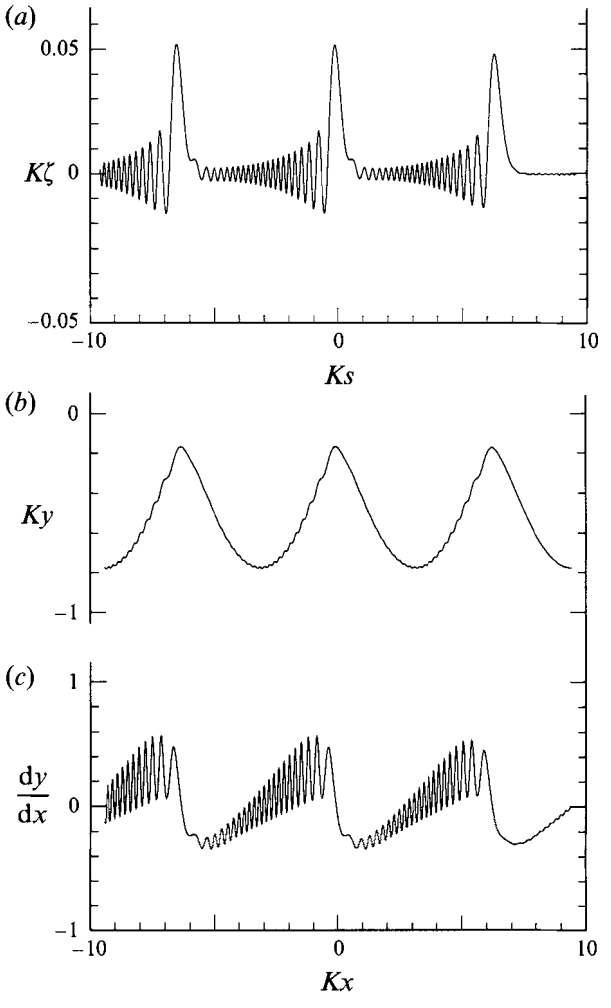

FIGURE 11. Computed profiles of (*a*) the normal displacement $\zeta(s)$, (*b*) the surface elevation $y(x)$, and (*c*) the surface gradient $\mathrm{d}y/\mathrm{d}x$, in the subcritical case $L = 8.0$ cm, $AK = 0.28$.

Figure 12 shows the dependence of the ripples on gravity wave steepness AK, keeping the wavelength L constant. We see there is a marked increase in the ripple amplitude as the critical wave steepness is approached. In fact only a slight increase in AK, from 0.28 to 0.30 for example, doubles the ripple steepness.

We note that the unlimited ripple amplitude as $AK \rightarrow (AK)_c$ is due to the vanishing of the denominator $D(\phi)$ in (7.3). (When $D(\phi')$ is under the integral sign, as in (7.4) the infinity is integrated out and the integral stays finite.) This goes back to our use of the WKB approximation, which is no longer valid near a wave caustic. In a higher approximation (see for example Shyu & Phillips 1990) the infinity would be avoided. However, we leave this for a future calculation.

8. Supercritical waves

When the Stokes waves are supercritical we can no longer take the integral in (7.1) over the whole wave. The infinite limit of integration must be replaced by s_1 where s_1 corresponds to a wave caustic. We now have, formally,

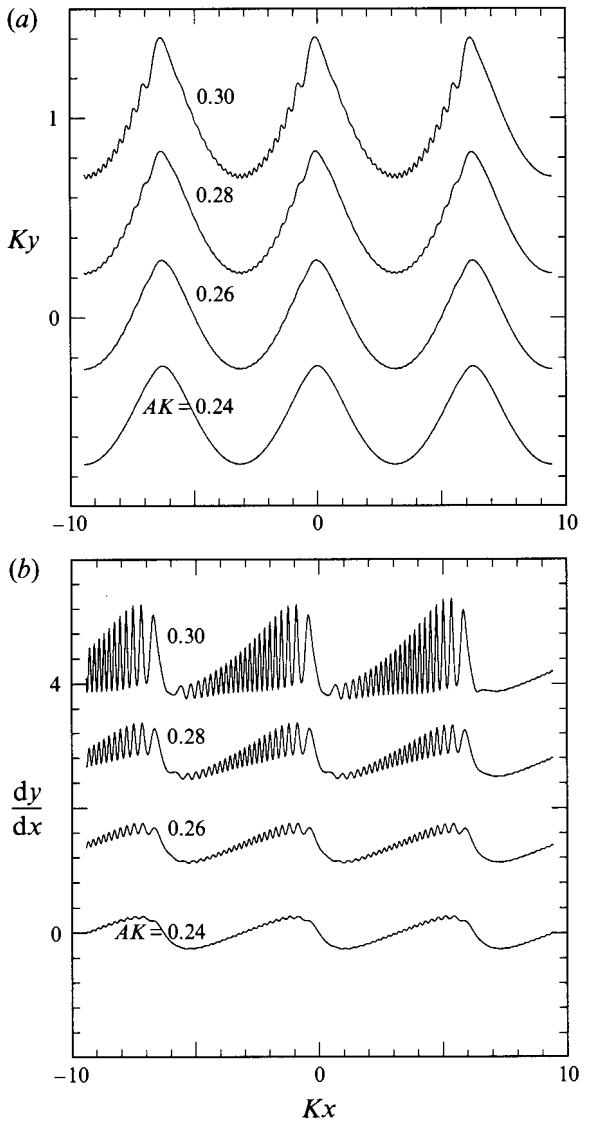

FIGURE 12. (*a*) Surface elevation $y(x)$, and (*b*) surface slopes $\mathrm{d}y/\mathrm{d}x$ when $L = 8.0$ cm and $AK = 0.24$, 0.26, 0.28 and 0.30 (all subcritical).

$$\zeta(s) = \int_{s_1}^{s} \frac{2T\kappa(s')\,\bar{F}(\phi)}{D(\phi)\,D(\phi')\,\bar{F}(\phi')} \sin(\bar{\theta}-\bar{\theta}')\,\mathrm{d}s', \tag{8.1}$$

where $\bar{\theta}$ and $\bar{F}$ are redefined so as to avoid singularities:

$$\left.\begin{aligned} \bar{\theta} &= \int_{s_1}^{s} k\,\mathrm{d}s, \\ \bar{F}(\phi) &= \exp\left(4\nu \int_{\phi_1}^{\phi} k^2/\Delta^2\,\mathrm{d}\phi\right), \end{aligned}\right\} \tag{8.2}$$

and hence

$$\zeta(s) = 2T\frac{\bar{F}(\phi)}{D(\phi)}[H(\phi)\cos\bar{\theta}\,G(\phi)\sin\bar{\theta}], \tag{8.3}$$

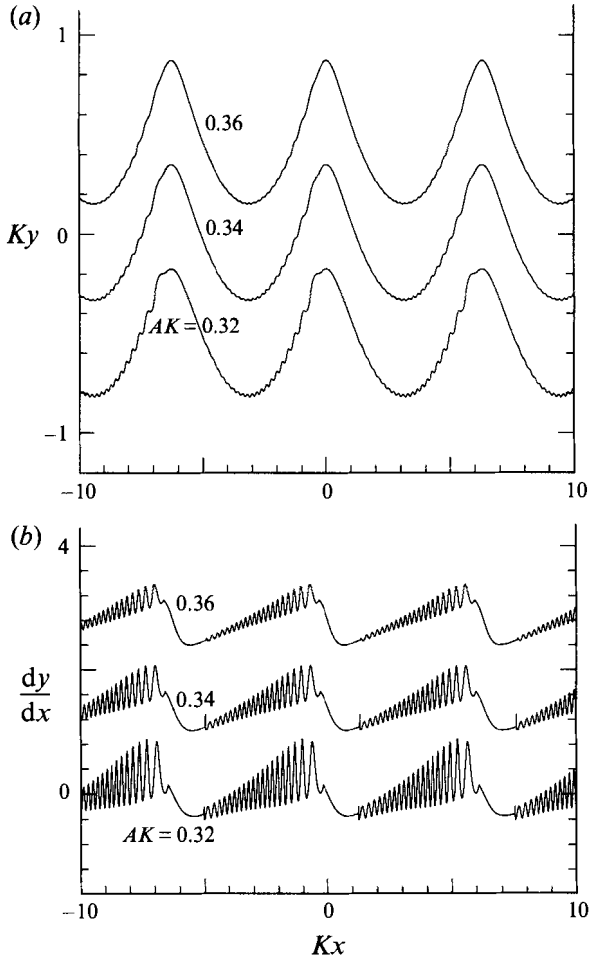

FIGURE 13. (*a*) Surface elevation $y(x)$ and (*b*) surface slopes $\mathrm{d}y/\mathrm{d}x$ when $L = 8.0$ cm and $AK = 0.32$, 0.34 and 0.36 (all supercritical).

where now

$$\left.\begin{aligned} G(\phi) &= \int_{\phi_1}^{\phi} \frac{\kappa(\phi')}{D(\phi')\,\bar{F}(\phi')\,U(\phi')} \cos\bar{\theta}'\,\mathrm{d}\phi', \\ H(\phi) &= \int_{\phi_1}^{\phi} \frac{\kappa(\phi')}{D(\phi')\,\bar{F}(\phi')\,U(\phi')} \sin\bar{\theta}'\,\mathrm{d}\phi'. \end{aligned}\right\} \tag{8.4}$$

Again the presence of $D(\phi')$ in the denominator of the integrand causes no problems, but when ϕ tends to the other caustic $D(\phi)$ tends to zero in (8.3), producing a spurious infinity. We therefore carry the calculation to within a small but positive distance from the caustic.

Physically, this implies that we do not treat realistically the neighbourhood of the second caustic s_2 (on the rear slope of the wave), and we neglect the reflection of the capillary–gravity waves as gravity waves at that point. In practice, though the amplitude of the capillary–gravity waves is much lower at the caustic than on the front of the waves, there may be some detectable capillary–gravity activity there.

The resulting calculations for supercritical Stokes waves of length $L = 8.0$ cm are shown in figure 13. The surface displacements (figure 13*a*) and slopes (figure 13*b*)

indicate that the surface becomes less rough as the steepness AK increases beyond the critical steepness. Together with figure 12 we may conclude that the capillary-gravity waves are of maximum amplitude for Stokes waves close to the critical steepness.

9. Conditions for validity

Before proceeding further it is appropriate to consider some conditions for validity of the above analysis.

In order that the basic Stokes wave shall be only slightly affected by surface tension it is necessary that

$$\eta^2 = TK^2/g \ll 1. \tag{9.1}$$

From table 2 we see that this restricts us to wavelengths L greater than about 5 cm, preferably 7 cm. Let us define η_0 by

$$\eta_0^2 = 4g_0^* T/U_0^4, \tag{9.2}$$

where a subscript 0 denotes, as before, the value at the wave crest $s = 0$. The condition for subcriticality may then be written

$$\eta_0 < 1. \tag{9.3}$$

Now on using the relations (3.4) and (3.5) we have

$$\eta_0 = 0.78\eta/\epsilon^2. \tag{9.4}$$

Hence the condition (9.3) is equivalent to

$$\eta \leqslant 1.28\epsilon^2. \tag{9.5}$$

In terms of the parameter η_0, the two wavenumbers k_1/k_2 at the wave crest are given by

$$k_1, k_2 = (U_0^2/2T)[1 \pm (1-\eta_0^2)^{1/2}], \tag{9.6}$$

cf. equation (4.3). In order that the short-wave approximation shall apply to the capillary waves at the crest, it is necessary that k_1 shall be large compared to the crest curvature R^{-1} where $R = 5.155\epsilon^2/K$ (see Longuet-Higgins & Fox 1977). Since by (9.6) k_1 is of order U_0^2/T this implies that

$$5.155\epsilon^2 \gg KT/U_0^2 = \eta^2/2\epsilon^2, \tag{9.7}$$

hence

$$\eta \ll 3.2, \tag{9.8}$$

consistently with (9.1).

Another basic condition is that near the crest we have

$$\frac{\partial U}{\partial s} \ll k_1 U, \tag{9.9}$$

(see §7). This implies

$$k_1 \gg \frac{1}{U_0^2}\frac{\partial}{\partial s}(\tfrac{1}{2}U_0^2) = \frac{1}{U_0^2}\frac{\partial}{\partial s}(gy). \tag{9.10}$$

But near the crest k_1 is of order U_0^2/T and $\partial y/\partial s$ is of order $\frac{1}{2}$. Hence the condition is satisfied if

$$\frac{U_0^2}{gT} \gg \frac{1}{2}, \tag{9.11}$$

that is to say

$$\eta_0^2 \ll 8g^*/g = 4.9, \tag{9.12}$$

which also is consistent with (9.3).

L(cm)	η^2	$(AK)_c$
5.0	0.1207	0.1846
6.0	0.0838	0.2445
7.0	0.0616	0.2837
8.0	0.0472	0.3112
9.0	0.0373	0.3313
10.0	0.0302	0.3467
12.0	0.0210	0.3683
15.0	0.0134	0.3826
20.0	0.0075	0.4054

TABLE 2. Values of $\eta^2 = TK^2/g$ and of the critical wave steepness $(AK)_c$ for different wavelengths L.

Note that when η_0^2 is small, then by (9.6)

$$k_2/k_1 \simeq \tfrac{1}{4}\eta_0^2 \ll 1, \tag{9.13}$$

so that the contributions of the two waves are dynamically well separated.

A second kind of criterion concerns the damping of the parasitic capillaries. For a clear understanding of the phenomenon it is desirable that the capillaries be effectively damped out over a distance comparable to one wavelength of the basic gravity wave. By §7 this implies that

$$\exp(-2\nu k_1^2 L/U) < 0.05, \tag{9.14}$$

say, or

$$2\nu k_1^2 L/U > 3. \tag{9.15}$$

Here L is the wavelength $(2\pi/K)$ and U is a representative value of the surface stream velocity. We may take U as the phase-speed $(g/K)^{1/2}$ and the capillary wavenumber k_1 as U^2/T. Then the condition (9.15) is equivalent to

$$K^{5/2} < \frac{4\pi}{3}\frac{\nu g^{3/2}}{T^2}. \tag{9.16}$$

In c.g.s. units the right-hand side of (9.15) equals 22 $\text{cm}^{-5/2}$, implying that

$$L = 2\pi/K > 11.7 \text{ cm}. \tag{9.17}$$

In other words, at basic wavelengths less than about 12 cm there may be appreciable interference between the capillary waves generated at adjacent crests of the basic wave.

10. Experiments by Cox (1958)

The first detailed measurements of the slopes of parasitic capillary waves were made by Cox (1958). His observations were made on plunger-generated waves in a short (6.1 m) wave tank both with and without wind. Although the direct effects of wind on the capillary waves may have been slight at most lower wind speeds we here confine attention to the observations where the wind speed was zero (see figure 14*a*).

The average period τ of the gravity waves is 0.202 s, but evidently the wave height was not completely uniform. This may have been due to reflection of energy from the far end of the tank, or to some inherent instability of the waves. Moreover, the time taken for the ripples to propagate over one wavelength of the gravity wave being longer than a wave period, the shorter waves were not always in a steady state.

Cox measured the surface slope at a fixed horizontal position as a function of time. The one enlarged record is his figure 11, here reproduced as figure 14(*b*). By drawing

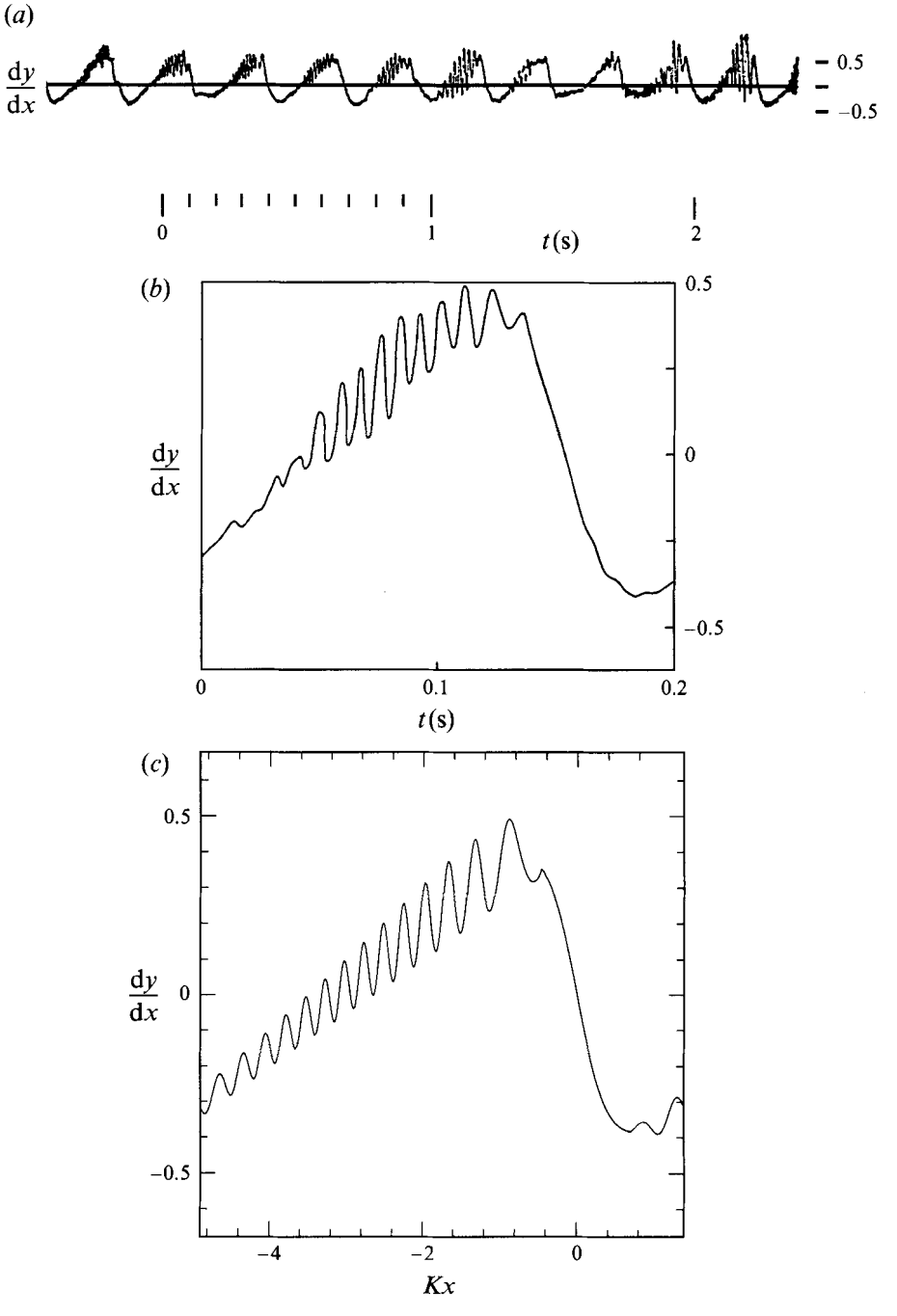

FIGURE 14. Time-trace of surface slope dy/dx in mechanically generated waves, period 0.202 s, without wind. (*a*) A sequence of waves; (*b*) details of the fourth wave in (*a*) [after Cox 1958]; (c) the wave slope dy/dx calculated by the method of §8 when $L = 6.5$ cm. $AK = 0.36$ and $\nu = 0.012$.

a smoothed curve through the experimental trace we infer a value 0.406 for the slope-amplitude of the underlying gravity wave (that is half the difference between the maximum and minimum slopes). Interpolating in table 1, we find this corresponds to a wave with steepness parameter $AK = 0.366$. The corresponding wave speed c is $1.069\, g\tau/2\pi$ and hence the wavelength $L = c\tau = 6.81$ cm approximately. (We have neglected the possible effect of surface tension on the overall wave speed.)

From figure 9 we see that the gravity wave is supercritical. The corresponding surface profile, from the theory of §8, is shown in figure 14(c), assuming that the kinematic viscosity ν has its expected value 0.012 cm^2 s^{-1}. When the position of the ripple crests in figure 14(b) and 14(c) are compared, it will be seen that they agree quite satisfactorily. As for the amplitudes, there are two points of disagreement. The measured amplitude of the first (i.e. right-hand) ripple is somewhat less than predicted. This is not surprising in view of our approximate treatment of the waves near a caustic. The second main discrepancy is that for negative slopes the measured capillary–gravity waves appear more highly damped than in the theory. This could be because the capillary–gravity wavetrain was unsteady and energy was still being propagated to the lower part of the longer wave. Note that for ripples, the ratio of the group velocity c_g to the phase velocity c is less than $\frac{3}{2}$, hence the velocity of energy propagation against the current is less than $\frac{1}{2}c$ and the time for the capillary wave energy to propagate over a distance $\frac{1}{2}L$ is greater than one wave period.

11. Observations by Perlin *et al.* (1993)

Perlin *et al.* (1993) observed plunger-generated waves at two fixed frequencies: 5.26 and 4.21 Hz. They measured essentially the surface displacement at a given instant of time, over a distance of a few wavelength from the wavemaker. From their figures 9 and 12 it is immediately clear that the capillary waves changed considerably over that distance. Generally, the further the gravity wave from the wavemaker, the smaller the amplitude of the ripples. It is therefore permissible to doubt whether the gravity waves were steady, since at finite amplitude a wavemaker generally creates higher harmonics of the gravity wave, which propagate freely over the fundamental wave. At the crest of the fundamental wave the higher harmonics are amplified by the orbital motion of the fundamental, as is well understood (see Longuet-Higgins & Stewart 1964) so that the wave crests are especially variable close to the wavemaker and take a few wavelengths to settle down. There may also be some capillary waves generated at the wavemaker itself, by the action of surface tension and viscosity.

Figure 15(a) is the profile of a 5.26 Hz wave shown as figure 7(a) of Perlin *et al.* (1993). Taking the wave height $2A$ as 0.47 cm and the wavelength L as 6.82 cm we have $AK = 2\pi A/L = 0.217$. Inserting these parameters in the analysis of §7 we find the surface profile shown in figure 15(b). Comparing this with figure 15(a) we see that the positions of the ripple crests correspond quite closely. The ripple amplitude is smaller than observed (by about 50%) near the crest of the wave, but is of about the same magnitude as observed in the wave trough. Reference to figure 10, at the same wavelength $L = 6.82$, suggests that there may well have been an overspill of energy from the previous wave.

We come now to the experiments at 4.21 Hz. Figure 11 of Perlin *et al.* represents the surface profile at a distance of 1–2 wavelengths from the wavemaker. From this we see that the wave height $2A$ was 0.82 cm and the wavelength L about 10.2 cm, giving $AK = 0.25$. The waves were therefore strongly subcritical. It is quite clear, however, that in their figure 11, which is used to compare with previous theory, the waves were

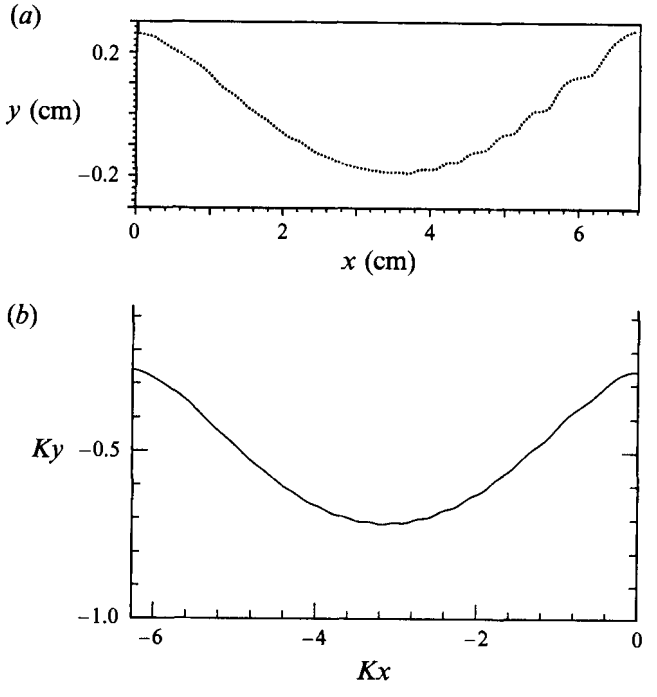

FIGURE 15. (*a*) The profile of a wave at 5.26 Hz as recorded by Perlin *et al.* (1957) figure 7(*a*). (*b*) The profile calculated by §7 with $L = 6.82$ cm, $AK = 0.227$.

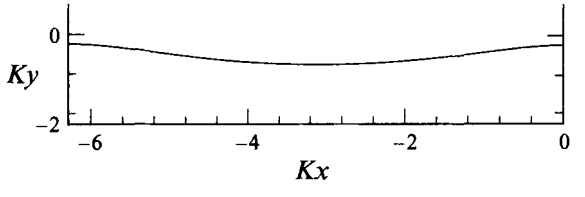

FIGURE 16. The theoretical profile for a wave with $L = 10.2$ cm, $AK = 0.25$, by the method of §7.

not yet steady. For on p. 617 they state, 'The lower-frequency gravity wavetrain experiences a more rapid decrease in the parasitic capillaries, which are almost non-existent by 2.5 wavelengths downstream.' In other words, if in figure 11 they had shown the wave profile at 2.5 wavelengths downstream where it was presumably more steady, the parasitic capillaries would have been negligible.

This is confirmed by inserting the above parameters for the waves in the analysis of §7, which yields the profile shown in figure 16. In this, the parasitic capillaries are indeed so small as to be practically invisible.

12. Observations by Ebuchi *et al.* (1987)

It is interesting to contrast the observations of Perlin *et al.* (1993) with those of Ebuchi *et al.* (1987), here reproduced as figure 17(*a*). The latter observations were made in the presence of a wind of 6 m s^{-1} and with a fetch of 6 m. The wavelength was about 10 cm, quite comparable with the measurements at 4.21 Hz by Perlin *et al.*, but the wave steepness was much greater, about 0.335. As shown by Ebuchi *et al.* the crests of the gravity waves were regions of high vorticity. In figure 17(*b*) we show the

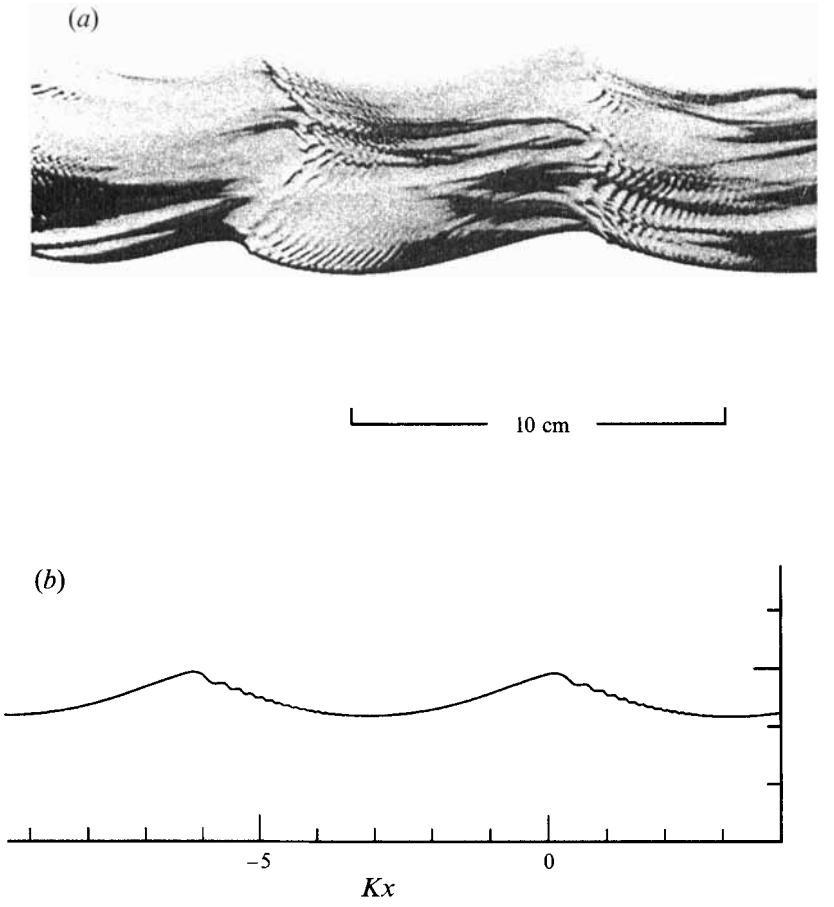

FIGURE 17. Waves generated by a wind of 6 m s^{-1} in a laboratory flume [from Ebuchi *et al.* 1987]. (*b*) Wave calculated by §7, with $L = 10.0$ cm, $AK = 0.36$.

capillary–gravity waves produced by an irrotational wave with $L = 10$ cm, $AK = 0.335$. The ripples are very similar to these shown in figure 17(*a*), there being about 20 ripples between the wave trough and the point on the profile corresponding to the toe of the roller.

As pointed out in Longuet-Higgins (1992), the main action of the wind in the experiments by Ebuchi *et al.* was to put energy into the gravity waves (perhaps mainly by normal pressure on the surface) and steepen them to the point where parasitic capillaries were generated. The high rate of damping of the capillary waves was shown to produce enough rectified vorticity to account for the turbulence in the gravity wave crests, and to sustain the crest 'roller'.

At still greater wavelengths (0.5–2.0 m) experiments by Duncan *et al.* (1994) have confirmed that the crest of a steep Stokes wave is inherently unstable, and tends to be thrown forward, in accordance with theoretical calculations by Longuet-Higgins, Cleaver & Fox (1994). This instability also contributes to the formation of a 'toe' or point of sharp curvature on the forward face of the wave, and hence the production of parasitic capillaries. A similar instability may contribute to the asymmetry of the crests in figure 17, at a shorter wavelength.

13. Discussion and conclusions

To render the calculations practicable we have made a number of significant approximations:

1. To a first approximation, the waves are assumed to be steady, irrotational gravity waves.

2. In the perturbation due to capillarity we have considered only the resonant capillary–gravity component. The gravity–capillary component and the localized 'transient' (see figure 7*a*) are both neglected.

3. The capillary–gravity waves are supposed linear (i.e. of small steepness) so that we may superpose the contributions arising from different parts of the free surface.

4. We use the WKB approximation except very close to the 'blocking points' or caustics, hence the neighbourhood of blocking points is not well represented. (This difficulty does not of course arise for subcritical waves.)

5. We have neglected the reaction of the capillary waves on the basic flow. In a second approximation this would have to be included.

6. We have assumed the flow is steady, although there is some evidence of unsteadiness in the experiments. The waves can only be steady in a first approximation; complete steadiness would require some input of energy from the wind, or a gradual decay of the gravity waves with horizontal distance.

Nevertheless our results reveal some of the essential physics of capillary wave generation: (*a*) They appear to originate from regions of sharp curvature of the (unperturbed) surface profile. (*b*) Stokes waves of a given wavelength L are two kinds: subcritical, in which the generation of parasitic capillaries can occur at all points of the surface, and supercritical, in which capillary–gravity generation occurs only in the wave troughs between two wave caustics. (*c*) The critical value $(AK)_c$ of the gravity wave steepness, dividing subcritical from supercritical waves, has been accurately calculated. (*d*) The amplitude of the parasitic capillaries, hence the damping of the gravity waves, is greatest when the gravity waves are close to their critical steepness, i.e. when $AK \simeq (AK)_c$. Evidently the damping of a Stokes wave is a highly nonlinear function of its steepness, as pointed out by Longuet-Higgins (1963).

The present theory accounts fairly well for the measurements of surface slopes by Cox (1958) especially taking into account the probable unsteadiness of the steep waves in his experiments. The theory also agrees with the observations by Perlin *et al.* (1993), although we have noted some discrepancies in their presentation of their own data (see §11, para 3). The experiments by Ebuchi *et al.* (1987) can also be accounted for. It is not possible to assess the data quoted by Ruvinsky *et al.* (1991) without further details of their experimental set-up. The generation of parasitic capillaries is a delicate phenomenon in which great experimental care is necessary.

The length of the gravity wave is a highly relevant parameter. For wavelengths L less than about 8 cm the overlap of capillary–gravity waves generated on adjacent gravity waves can be appreciable for subcritical waves. In the supercritical case we would expect to see some capillary-wave activity near the caustic on the rear face of the Stokes wave, as well as on the front face. For wavelengths L above 10 cm the broadness of the wave crest tends to iron out the capillary–gravity waves, in the subcritical case. However, natural instabilities of the wave crest (Longuet-Higgins *et al.* 1994) tend to produce a sharp discontinuity of slope on the forward face, leading to a very localized source of parasitic capillaries. This process is helped by the generation of vorticity by the capillaries themselves (Longuet-Higgins 1992). It is desirable to consider further the effects of viscosity on steep gravity waves, through the production of vorticity by the

parasitic capillaries. The possibility of steady solutions with input of energy from the wind should be investigated. Calculations of the present type could also be extended to unsteady Stokes waves, such as those occurring in focused wave packets or in wave groups, and ultimately to waves in three dimensions.

The present work has been supported by the Office of Naval Research under ONR Grant N00014-94-1-0008.

REFERENCES

CHANG, J. H., WAGNER, R. N. & YUEN, H. C. 1978 Measurement of high frequency capillary waves on steep gravity waves. *J. Fluid Mech.* **86**, 401–413.

CHEN, B. & SAFFMAN, P. G. 1979 Steady gravity–capillary waves on deep water – I. Weakly nonlinear waves. *Stud. Appl. Maths* **60**, 183–210.

CHEN, B. & SAFFMAN, P. G. 1980 Steady gravity–capillary waves on deep water – II. Numerical results for finite amplitude. *Stud. Appl. Maths* **62**, 95–111.

COX, C. S. 1958 Measurements of slopes of high-frequency wind waves. *J. Mar. Res.* **16**, 199–225.

CRAPPER, G. D. 1970 Non-linear capillary waves generated by steep gravity waves. *J. Fluid Mech.* **40**, 149–159.

DAVIES, T. V. 1951 The theory of symmetrical gravity waves of finite amplitude. I. *Proc. R. Soc. Lond.* **208**, 475–486.

DUNCAN, J. H., PHILOMIN, V., QIAO, H. & KIMMEL, J. 1994 The formation of a spilling breaker. *Phys. Fluids* **6**, S2.

EBUCHI, N., KAWAMURA, H. & TOBA, Y. 1987 Fine structure of laboratory wind–wave surfaces studied using an optical method. *Boundary-Layer Met.* **39**, 133–151.

JÄHNE, B. & RIEMER, K. 1990 Two-dimensional wave number spectra of small scale water surface waves. *J. Geophys. Res.* **95**, 11 531–11 546.

LAMB, H. 1932 *Hydrodynamics*, 6th ed. Cambridge University Press, 738 pp.

LONGUET-HIGGINS, M. S. 1963 The generation of capillary waves by steep gravity waves. *J. Fluid Mech.* **16**, 238–159.

LONGUET-HIGGINS, M. S. 1985*a* Bifurcation in gravity waves. *J. Fluid Mech.* **151**, 457–475.

LONGUET-HIGGINS, M. S. 1985*b* Accelerations in steep gravity waves. *J. Phys. Oceanogr.* **15**, 1570–1579.

LONGUET-HIGGINS, M. S. 1987 The propagation of short surface waves on longer gravity waves. *J. Fluid Mech.* **177**, 293–306.

LONGUET-HIGGINS, M. S. 1992 Theory of weakly damped Stokes waves: a new formulation and its physical interpretation. *J. Fluid Mech.* **235**, 319–324.

LONGUET-HIGGINS, M. S. & CLEAVER, R. P. 1994 Crest instabilities of gravity waves. Part 1. The almost-highest wave. *J. Fluid Mech.* **258**, 115–129.

LONGUET-HIGGINS, M. S., CLEAVER, R. P. & FOX, M. J. H. 1994 Crest instabilities of gravity waves. Part 2. Matching and asymptotic expansion. *J. Fluid Mech.* **259**, 333–344.

LONGUET-HIGGINS, M. S. & FOX, M. J. H. 1977 Theory of the almost-highest wave: the inner solution. *J. Fluid Mech.* **80**, 721–741.

LONGUET-HIGGINS, M. S. & FOX, M. J. H. 1978 Theory of the almost-highest wave. Part 2. Matching and analytic extension. *J. Fluid Mech.* **85**, 769–786.

LONGUET-HIGGINS, M. S. & STEWART, R. W. 1964 Radiation stresses in water waves; a physical discussion, with applications. *Deep-Sea Res.* **11**, 529–562.

PERLIN, M., LIN, H. & TING, C.-L. 1993 On parasitic capillary waves generated by steep gravity waves: an experimental investigation with spatial and temporal measurements. *J. Fluid Mech.* **255**, 597–620.

PHILLIPS, O. M. 1981 The dispersion of short wavelets in the presence of a dominant long wave. *J. Fluid Mech.* **107**, 465–485.

RUVINSKY, K. D., FELDSTEIN, F. I. & FREIDMAN, G. I. 1991 Numerical simulations of the quasi-

stationery stage of ripple excitation by steep gravity–capillary waves. *J. Fluid Mech.* **230**, 339–353.

RUVINSKY, K. D. & FREIDMAN, G. I. 1981 On the generation of capillary–gravity waves by steep gravity waves. *Izv. Atmos. Ocean. Phys.* **17**, 548–553.

SCHWARTZ, L. W. & VANDEN-BROECK, J.-M. 1979 Numerical solution of the exact equations for capillary–gravity waves. *J. Fluid Mech.* **95**, 111–139.

SHYU, J.-H. & PHILLIPS, O. M. 1990 The blockage of gravity and capillary waves by longer waves and currents. *J. Fluid Mech.* **217**, 115–141.

WATSON, K. M. & MCBRIDE, J. B. 1993 Excitation of capillary waves by longer waves. *J. Fluid Mech.* **250**, 103–119.

YERMAKOV, S. A., RUVINSKY, K. D. & SALASHIN, S. G. 1988 Local correlation of the characteristics of ripples on the crest of capillary gravity waves with their curvature. *Izv. Atmos. Ocean. Phys.* **24**, 561–563.